Resonant tunneling through quantum-dot arrays

Guanlong Chen,* Gerhard Klimeck,† and Supriyo Datta
School of Electrical Engineering, Purdue University, West Lafayette, Indiana 47907

Guanhua Chen‡ and William A. Goddard III
Material and Molecular Simulation Center, Beckman Institute, California Institute of Technology, Pasadena, California 91125
(Received 3 June 1994)

We apply the Hubbard Hamiltonian to describe quantum-dot arrays weakly coupled to two contacts. Exact diagonalization is used to calculate the eigenstates of the arrays containing up to six dots and the linear-response conductance is then calculated as a function of the Fermi energy. In the atomic limit the conductance peaks form two distinct groups separated by the intradot Coulomb repulsion, while in the band limit the peaks occur in pairs. The crossover is studied. A finite interdot repulsion is found to cause interesting rearrangements in the conductance spectrum.

Transport through a single quantum dot weakly coupled to two contacts has been the subject of much experimental and theoretical work,[1–4] and a fairly clear picture has emerged. Relatively little work has been done on arrays of quantum dots, though it now seems feasible to fabricate such structures.[5] Most theoretical work on arrays has been based on the *RC* model which neglects coherence between individual dots in the array.[6] However, it is expected that in semiconductor quantum-dot arrays such interdot coherence will play an important role in determining the transport properties. The purpose of this paper is to present theoretical results for the conductance of coherent arrays as a function of the Fermi energy, $G(E_F)$.

A single quantum dot behaves as an artificial atom in its charge and energy quantizations[1] and is often described by the Anderson Hamiltonian,[4] in which there is a finite Coulomb repulsion between any two electrons on the dot. For an array of quantum dots with phase coherence, each dot can be viewed as an artificial atom with intradot Coulomb repulsion (as in Anderson model), and electrons hop between nearest neighbor dots. It seems reasonable then to model an array of quantum dots using the Hubbard Hamiltonian[7] characterized mainly by two parameters: the intradot charging energy (U) and the interdot coupling matrix element (t). Our approach is to calculate the many-body eigenstates of the array (isolated from the contacts) by exact diagonalization[8] and then to incorporate the effect of the contacts through a rate equation as done by Beenakker[3] for single dots. This treatment of the contacts should be accurate as long as the temperature is higher than the Kondo temperature. We have studied arrays containing $N = 2, 3, \ldots$ up to six dots, and find that (1) in the atomic limit ($t < U$) the peaks in the conductance $G(E_F)$ form two distinct symmetric groups separated by U and (2) in the band limit ($t > U$) the peaks occur in pairs separated by order of U. Thus even such short arrays exhibit properties reminiscent of the infinite Hubbard chain. Interstingly, we find that the inclusion of inelastic processes within the array does not significantly affect the results. It might thus be possible to study various aspects of the Hubbard model using such artificial quantum-dot arrays.

Real arrays can be expected to have two main deviations from the ideal Hubbard model. First, in addition to the intradot Coulomb repulsion there will exist a certain degree of interdot repulsion. Second, individual dots will be invariably "detuned" from each other to some extent.[9] Both these aspects are readily incorporated in our model, and we find that they have a noticeable effect on the conductance spectrum. Interdot repulsion destroys the symmetry between the two groups of peaks which we identified as the upper and the lower Hubbard bands. Detuning tends to localize the electron states, thus suppresses the conduction peaks. The effects of detuning have been presented in a separate publication.[10]

Consider a one-dimensional (1D) array of N coupled dots, indexed from left to right as 1–N, described by the Hamiltonian H,

$$\begin{aligned} H = & \sum_{\alpha;k\in L,R} \epsilon_{k\alpha} c^{\dagger}_{k\alpha} c_{k\alpha} + \sum_{\alpha;i=1}^{N} \epsilon_{i\alpha} c^{\dagger}_{i\alpha} c_{i\alpha} + \sum_{i=1}^{N} U_i n_{i\uparrow} n_{i\downarrow} \\ & + \sum_{i=1}^{N-1} (t_i c^{\dagger}_{i\alpha} c_{i+1\alpha} + \text{c.c.}) + \sum_{\alpha,\beta;i=1}^{N-1} W_i n_{i\alpha} n_{i+1\beta} \\ & + \sum_{\alpha;k\in L} (V^L_{k\alpha} c^{\dagger}_{1\alpha} c_{k\alpha} + \text{c.c.}) \\ & + \sum_{\alpha;k\in R} (V^R_{k\alpha} c^{\dagger}_{N\alpha} c_{k\alpha} + \text{c.c.}). \end{aligned} \tag{1}$$

In Eq. (1), $\epsilon_{k\alpha}$ and $\epsilon_{i\alpha}$ are energy levels in leads and the ith dot of the array, respectively, with α being the spin index. U_i is the intradot repulsion of the ith dot, while W_i and t_i are the interdot repulsion and the interdot coupling between the ith dot and its right neighbor [the $(i+1)$th dot]. The tunneling matrix element $V^L_{k\alpha}$ ($V^R_{k\alpha}$) connects dot 1 (dot N) to the left (right) lead. We assume two spin-degenerate levels on each dot.

We treat the whole array as a *single* quantum system and calculate its many-body eigenstates by exact diagonalization. The demand on computing power grows factorially with the number of states. Arrays containing up

to six dots (12 states) were studied. Once the eigenstates are known, the conductance is calculated from the relation

$$G = \left(\frac{e^2}{kT}\right) \sum_n \sum_{ij} \frac{\Gamma^L_{n,ij}\Gamma^R_{n,ij}}{\Gamma^L_{n,ij} + \Gamma^R_{n,ij}} \times P^{\rm eq}_{n,i}[1 - f_{FD}(\epsilon_{n,i} - \epsilon_{n-1,j} - \mu)]. \quad (2)$$

In Eq. (2), $\epsilon_{n,i}$ is the energy of many-body state (n,i), the ith of the n-particle states, $\Gamma^{L(R)}_{n,ij}$ are the transition rates between state (n,i) and $(n-1,j)$ by losing or getting one electron through the left (right) lead, and $P^{\rm eq}_{n,i}$ is the occupation probability of state (n,i) at equilibrium,

$$P^{\rm eq}_{n,i} = (1/Z)\exp[-(1/kT)(\epsilon_{n,i} - n\mu)], \quad (3)$$

where Z is the partition function

$$Z = \sum_{n,i} \exp\left[-\frac{1}{kT}(\epsilon_{n,i} - n\mu)\right]. \quad (4)$$

Equation (2) is basically the same as those used in Ref. 3 for single dots. The only difference is that the eigenstates of an array have a more complicated spatial structure and this has to be taken into account when calculating the transition rates $\Gamma^{L(R)}_{n,ij}$ in terms of the transition rate Γ out of a single dot into a lead.[15]

Equation (2) is valid if there is no inelastic scattering within the array. For comparison we also evaluated the conductance in the opposite limit when the inelastic scattering is so strong that the array is in local equilibrium.[3] No significant differences were found. For this reason, we believe that inelastic processes within the dot have no effect on our results. It is important to mention that the approach we use here is valid only when the lead coupling is small compared to the thermal energy, otherwise one cannot neglect the leads when calculating the many-body eigenstates of the array.

To start with we assume that the array is uniform, i.e., $\epsilon_{i\alpha} = \epsilon_0$, $U_i = U$, $t_i = t$, $V^L_{k\alpha} = V^R_{k\alpha}$, and no interdot repulsion $W_i = 0$ $(i = 1,2,...,N)$. First we examine a two-dot system, and assume low temperature and small interdot coupling $(U \gg t)$, so that excited states and second order interdot coupling $O(t^2)$ can be neglected. Consider what happens as we raise the Fermi energy starting with zero electrons in the array. The first electron coming into the system occupies the bonding state, which has an energy $\epsilon_0 - t$. When a second electron comes in, the two electrons tend to localize at different sites to avoid the intradot repulsion U; therefore the ground state energy is roughly $2\epsilon_0 + O(t^2)$. After half filling, the third electron has to overcome the repulsion U, and with the same bonding scheme, the system is at energy $3\epsilon_0 + U - t$. Finally, the system with four electrons has an energy $4\epsilon_0 + 2U$. As one sweeps up the Fermi energy, the two-dot system undergoes $0 \to 1, 1 \to 2, 2 \to 3$, and $3 \to 4$ particle transitions at $\epsilon_0 - t, \epsilon_0 + t + O(t^2), \epsilon_0 + U - t + O(t^2)$, and $\epsilon_0 + U + t$, respectively, according to Eq. (3). At the transition points, the system is able to fluctuate between n and $n+1$ $(n = 0,1,2,3)$ particle states, allowing electrons to tunnel in and out of the array, giving rise to a peak in the conductance. For a two-dot array the eigenstates can be expressed analytically, and the second order interdot coupling $O(t^2)$ turns out to be $-2t^2/U$. For longer chains, the many-body states are solved numerically, and the peak positions can be determined by physical arguments similar to those given above.

The conductance spectrum for chains containing two to six dots in the atomic limit is shown in Figs. 1(a)–1(e) ($U = 5$ meV, $t = 1$ meV). Figure 1(a) (dashed curve) also shows the number of electrons in the array, where we see that each conductance peak corresponds to one electron filling into the system. The conductance has two symmetric groups separated by roughly the intradot repulsion U, and each group has a number of peaks equal to the number of dots in the array. The conductance spectrum starts to reflect the formation of Hubbard bands as the chain gets longer. At higher temperature

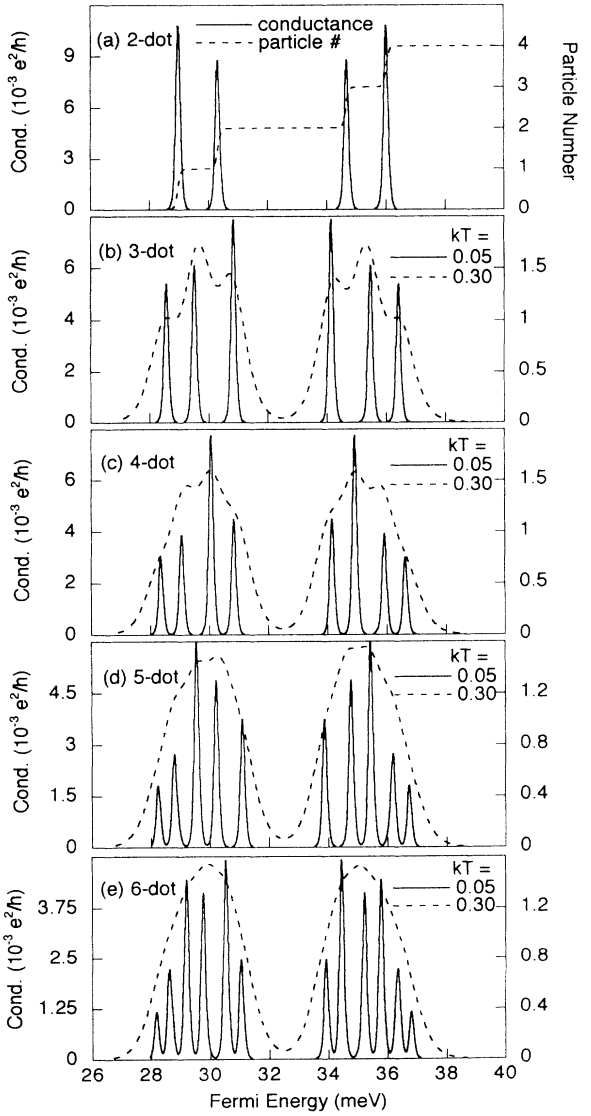

FIG. 1. Linear-response conductance vs Fermi energy in the atomic limit ($U = 5$, $t = 1$) for (a) two-dot, (b) three-dot, (c) four-dot, (d) five-dot, and (e) six-dot chains. In (a), the solid and dashed curves show conductance and particle transition at $kT = 0.05$. In (b)–(e), the solid and dashed curves show conductance at $kT = 0.05$ and 0.3, respectively. In all figures, the solid curves refer to the left y-axis scales, while the dashed curves refer to the right y-axis scales. $\epsilon = 30$, $W = 0$, $\Gamma = 0.001$. Energy units are in meV.

(dashed lines), the multiple-peak features are smeared out by thermal broadening and only the two "bands" separated by U remain visible. The amplitudes of the peaks are determined by how well the initial and final states of the particle transition couple to each other through the leads. It is hard to give simple physical arguments explaining the relative amplitudes of the peaks. Nevertheless, the upper and lower groups are symmetric, due to the electron-hole symmetry, i.e., for every state below the half filling, there exists an electron-hole complement state above the half filling, and vice versa.

We also studied cases in which the interdot coupling is comparable to or greater than the intradot repulsion. Figure 2 shows the conductance of three-dot and six-dot chains with interdot coupling $t = 5$ meV and intradot repulsion $U = 1$ meV or 5 meV. In this band limit, conductance peaks occur in pairs. Here the interdot coupling t determines the separation between different pairs of peaks, while the intradot repulsion U causes the splitting between the two peaks within a pair. It can be shown that each pair corresponds to the tunneling of two electrons with opposite spin. In the limit of zero intradot repulsion ($U \to 0$), the two peaks merge into one as we would expect from a one-particle picture. For small U, the pairing feature is washed out by thermal broadening. Hence, at high temperatures one sees single peaks instead, which are similar to that of noninteracting tunneling.[5] The insets of Figs. 2(b) and 2(d) depict the conductance peak loci of three-dot and six-dot chains as a function of the interdot coupling at low temperatures, where excited states can be neglected. The insets demonstrate the evolution from "two-band" structures into patterns of paired peaks with increasing the interdot coupling. This evolution corresponds to the crossover of the Hubbard model from the atomic limit ($U \gg t$) to the band limit ($U \ll t$), which is of special interest in the high-T_c superconducting systems.[11–13]

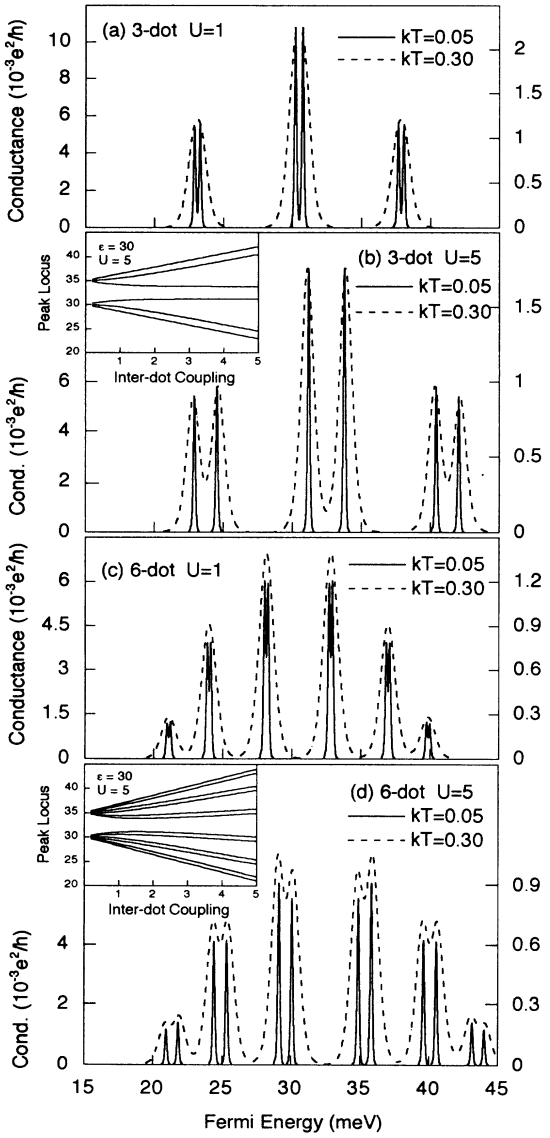

FIG. 2. Linear response conductance vs Fermi energy in the band limit ($t = 5$). (a) Three-dot, $U = 1$; (b) three-dot, $U = 5$; (c) six-dot, $U = 1$; and (d) six-dot, $U = 5$ with $kT = 0.05$ and 0.3. The solid and dashed curves refer to the scales of the left and right y axes, respectively. The insets of (b) and (d) show the conductance peak loci of three-dot and six-dot chains with $U = 5$ at the variance of interdot coupling. $\epsilon = 30, W = 0, \Gamma = 0.001$. Energy units are in meV.

So far we have neglected interdot repulsion. However, this could be significant in real quantum-dot arrays. To illustrate the effect of interdot repulsion, we show the atomic-limit conductance spectrum of a six-dot chain in the presence of moderate interdot repulsion ($W = 1$ meV) in Fig. 3. The interdot repulsion changes the many-body ground state energies as well as their compositions, and the change is amplified as the number of electrons is increased. Thus the interdot repulsion causes more significant changes in the upper Hubbard band than the lower one, and the symmetry is broken between the upper and lower bands in the conductance spectrum. In the following, we take a three-dot chain to show explicitly why peak amplitudes change in the presence of interdot repulsion.

In a three-dot system, there are six single-particle states: (1) dot 1, spin up; (2) dot 1, spin down; (3) dot 2, spin up; (4) dot 2, spin down; (5) dot 3, spin up; (6) dot 3, spin down. We index the six states in this order. For example, $|010100\rangle$ simply denotes a many-body state that has two spin-down electrons, one at dot 1 and another at dot 2. With no interdot repulsion, the six states $|011111\rangle$, $|101111\rangle$, $|110111\rangle$, $|111011\rangle$, $|111101\rangle$, and $|111110\rangle$ are degenerate and have the same probability in the five-particle ground state. However, with finite interdot repulsion W, the energies of the four states with the hole at end dots ($|011111\rangle$, $|101111\rangle$, $|111101\rangle$, and $|111110\rangle$) increase by $6W$, while those of the two states with the hole in the middle dot ($|110111\rangle$ and $|111011\rangle$) increase only by $4W$. Therefore with interdot repulsion the new ground state is mainly composed of $|110111\rangle$ and $|111011\rangle$, which cannot make transitions to the six-particle state $|111111\rangle$ through the leads. As a result, the $5 \to 6$ conductance peak is greatly suppressed. On the other hand, the one-particle states, which are the electron-hole complement states of the five-particle states when there is no interdot repulsion, experience no interdot repulsion and remain unchanged. Therefore the electron-hole symmetry breaks and the two conductance groups become distinct.

The nonmonotonic temperature dependence of the

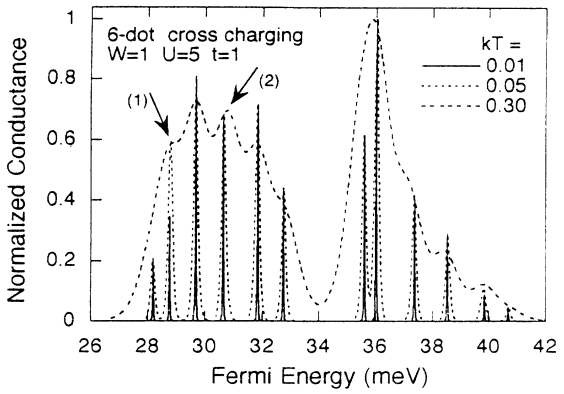

FIG. 3. Atomic-limit conductance spectrum of a six-dot chain with interdot repulsion ($W = 1$). The arrows indicate the nonmonotonic temperature dependence of the peaks. $\epsilon = 30, U = 5, \Gamma = 0.001, t = 1$, and $kT = 0.01, 0.05, 0.30$. Energy units are in meV.

conductance peak is noteworthy. It is visible in Fig. 3 that raising temperature not only broadens the peak widths and reduces the heights, but changes the relative amplitudes (see arrow 1) and moves peak positions (see arrow 2) as well. This nonmonotonic behavior is due to the fact that excited states are populated and participate in the transport at high temperatures. At the same time, the coupling of the leads to the excited states could be very different from the coupling to the ground state. The same nonmonotonic temperature dependence is equally present at zero interdot repulsion cases, which is quite visible in Fig. 1(b). The nonmonotonic behavior in dot arrays is similar to that of a single dot with strong energy dependence of lead coupling.[4]

We have studied 1D arrays of quantum dots, and it is demonstrated that some features of the Hubbard model can be probed by the conductance measurements. Similar conclusions should apply in higher dimensions. 2D quantum-dot arrays might be especially interesting because of relevance to high-T_c superconductors. Transport studies of quantum-dot arrays could shed light on our understanding of correlated transport and the Hubbard model. We hope that this paper will motivate both experimental and further theoretical studies on the interplay between quantum-dot arrays and the Hubbard model.

The authors would like to thank M. P. Anantram and Dr. R. Lake for helpful discussions. The work at Purdue was supported by the National Science Foundation (Grants Nos. ECS-9201446 and ECS-9110980) and the work at Caltech was supported by the NSF (Grant No. CHE91-100284) and by grants to the MSC (NSF, Allied-Signal, Asahi Glass, Asahi Chemical, BF Goodrich, Chevron, Xerox, and the Beckman Institute). We have recently found a similar work by Stafford and Das Sarma,[14] which calculated the capacitance spectrum of an array of quantum dots.

* Present address: Beckman Institute, MC-251, 405 North Mathews Avenue, University of Illinois, Urbana, IL 61801.
† Present address: Eric Jonsson School of Engineering and Computer Science, University of Texas at Dallas, Richardson, Texas 75083-0688.
‡ Present address: Department of Chemistry, University of Rochester, Rochester, NY 14627.

[1] M. A. Kastner, Phys. Today **46** (1), 24 (1993).
[2] U. Meirav, M. A. Kastner, and S. J. Wind, Phys. Rev. Lett. **65**, 771 (1990); B. Su, V. J. Goldman, and J. E. Cunningham, Science **255**, 313 (1992).
[3] C. W. J. Beenakker, Phys. Rev. B **44,** 1646 (1991).
[4] Y. Meir, N. S. Wingreen, and P. A. Lee, Phys. Rev. Lett. **66**, 3048 (1991).
[5] R. J. Haug, J. M. Hong, and K. Y. Lee, Surf. Sci. **263**, 415 (1992); M. Tewordt *et al.*, Appl. Phys. Lett. **60**, 595 (1992); L. P. Kouwenhoven *et al.*, Phys. Rev. Lett. **65**, 361 (1990).
[6] P. Delsing, in *Single Charge Tunneling*, edited by H. Grabert and M. H. Devoret (Plenum, New York, 1992); L. I. Glazman and V. Chandrasekhar, Europhys. Lett. **19**, 623 (1992); A. A. Middleton and N. S. Wingreen, Phys. Rev. Lett. **71**, 3198 (1993).
[7] J. Hubbard, Proc. R. Soc. London Ser. A **276,** 238 (1963); **281,** 401 (1964).
[8] E. Dagotto, A. Moreo, F. Ortolani, J. Riera, and D. J. Scalapino, Phys. Rev. Lett. **67,** 1918 (1991); E. Kaxiras and E. Manousakis, Phys. Rev. B **37**, 656 (1988).
[9] With the gate metal placed close to a dot, a conduction electron induces its image charge mainly in the gate, thereby greatly reducing the interdot Coulomb repulsion. The quantum-dot dimensions and interdot coupling are better controlled in vertical structures than in lateral structures.
[10] Gerhard Klimeck, Guanlong Chen, and Supriyo Datta, Phys. Rev. B **50**, 2316 (1994).
[11] J. G. Bednorz and K. A. Müller, Z. Phys. B **64**, 189 (1986); C. W. Chu *et al.*, Phys. Rev. Lett. **58**, 405 (1987).
[12] P. W. Anderson, Science **235**, 1196 (1987); V. J. Emery, Phys. Rev. Lett. **58**, 2794 (1987); J. R. Schrieffer, X.-G. Wen, and S.-C. Zhang, *ibid.* **60**, 944 (1988).
[13] G. Chen and W. A. Goddard, Science **239**, 899 (1988); H. Q. Ding, G. H. Lang, and W. A. Goddard, Phys. Rev. B **46**, 2933 (1992); G. Shirane *et al.*, Phys. Rev. Lett. **59**, 1613 (1987); P. A. Lee and N. Read, *ibid.* **58**, 2691 (1987).
[14] C. A. Stafford and S. Das Sarma, Phys. Rev. Lett. **72**, 3590 (1994).
[15] Gerhard Klimeck, Ph.D. thesis, Purdue University, 1994.